RAA 2017 Vol. **17** No. **9**, 92 (12pp) doi: 10.1088/1674–4527/17/9/92

http://www.raa-journal.org *http://iopscience.iop.org/raa*

Research in Astronomy and Astrophysics

Supernova neutrinos in a strangeon star model

Mao Yuan[1], Ji-Guang Lu[2], Zhi-Liang Yang[1], Xiao-Yu Lai[3] and Ren-Xin Xu[2,4]

[1] Department of Astronomy, Beijing Normal University, Beijing 100875, China; *ym@mail.bnu.edu.cn*
[2] School of Physics, Peking University, Beijing 100871, China
[3] School of Physics and Engineering, Hubei University of Education, Wuhan 430205, China
[4] Kavli Institute for Astronomy and Astrophysics at Peking University, Beijing 100871, China

Received 2017 January 9; accepted 2017 May 2

Abstract The neutrino burst detected during supernova SN 1987A is explained in a strangeon star model, in which it is proposed that a pulsar-like compact object is composed of strangeons (*strangeon*: an abbreviation for "strange nucleon"). A nascent strangeon star's initial internal energy is calculated, with the inclusion of pion excitation (energy around 10^{53} erg, comparable to the gravitational binding energy of a collapsed core). A liquid-solid phase transition at temperature $\sim 1-2$ MeV may occur only a few tens of seconds after core collapse, and the thermal evolution of a strangeon star is then modeled. It is found that the neutrino burst observed from SN 1987A can be reproduced in such a cooling model.

Key words: stars: neutron — supernovae: individual (SN 1987A) — neutrinos

1 INTRODUCTION

The state of dense baryonic matter compressed during a supernova is not yet well understood because of the non-perturbative nature of the fundamental strong interaction, but it is popularly speculated that those compact stars are composed of nucleons (this kind of matter should actually be neutron rich because of the weak interaction, thus we usually call them neutron stars). However, it has already been proposed that these compact stars could be composed of strangeons, formerly known as quark-clusters or strange clusters (Xu 2003). Strangeon is actually an abbreviation for "strange nucleon," in which the constituent quarks can take the form of three flavors (up, down and strange) rather than two flavors for nucleons. Both normal nuclear and strangeon matter are self-bound by residual color interaction, so we may simply call a strangeon star (SS) a gigantic nucleus with strangeness.

Because of the massive (and thus non-relativistic) nature of strangeons and the short-distance repulsive force between them (an analogy of the nuclear hard core), the equation of state for strangeon matter is very stiff (Lai & Xu 2009) so that observations of two-solar mass pulsars (Demorest et al. 2010; Antoniadis et al. 2013) can be naturally explained. Strangeon matter would be solidified when its temperature is much lower than the residual interaction energy in-between (Dai et al. 2011), and pulsar glitches, with or without X-ray enhancement, can be understood in the regime of a starquake since the associated energy release depends on spin frequency in the solid SS model (Zhou et al. 2014).

In addition, the quake-induced release of both gravitational and elastic energy could be meaningful for anomalous X-ray pulsars and soft gamma-ray repeaters (Xu et al. 2006; Tong 2016). Because of the strangeness barrier on the stellar surface, the optical/ultraviolet excess of an X-ray dim isolated neutron star could then be understood by including free-free emission from an SS atmosphere (Wang et al. 2017). An SS could be spontaneously magnetized due to ferromagnetic transition of electrons (Lai & Xu 2016b), and some small glitches could be the results of collisions between the SS and strangeon nuggets (Lai & Xu 2016a). Despite these successes listed above, a general question arises: Is it possible to understand the neutrino burst observed during SN 1987A in the regime of an SS?

This is the question we are attempting to answer in this paper. Normal 2-flavor baryonic matter could be transformed into strangeon matter through strangeonization during a compression process. Similar to the neutronization process of $e + p \rightarrow n + \nu_{\rm e}$, a strangeonization process of $(u, d) \rightarrow (u, d, s)$ will also significantly kill off electrons and hence produce strange "nucleons,"

i.e., strangeons. A strangeon is a cluster of quarks with quark number $N_{\rm q}$ (probably 6, 9, 12 or 18). Being different from a strange quark star (SQS), as mentioned above, an SS could be converted to a solid star from a liquid one, with melting temperature $T_{\rm m} \sim$ MeV (Dai et al. 2011). Namely, after a phase transition, the whole SS could be in a solid state during its cooling process.

A photon-driven mechanism would work for both an SQS and an SS (e.g., Chen et al. 2007), alleviating the difficulty of a traditional neutrino-driven supernova (Thompson et al. 2003). Due to extremely high temperatures, significant numbers of neutrinos are radiated during a photon-driven supernova. The total photon energy released could be as much as $\sim 10^{52}$ erg according to our calculations below, but neutrinos still take away almost all of the gravitational energy, $\sim 10^{53}$ erg. In contrast to the conventional neutrino-driven model, neutrinos are usually trapped in a nascent SS due to high opacity caused by coherent scattering off strangeons, which means that an SS's "neutrinosphere" could be the same scale as that of a proto-SS. In this scenario, the neutrino emissivity of the SS depends on the temperature of the whole nascent SS, rather than on the thin layer of a proto-SS. Is it possible to test the scenario through neutrino observation? Luckily, in 1987 a neutrino burst in a core collapse supernova, SN 1987A, was detected by three detectors, Kamiokande-II (Hirata et al. 1987), Irvine-Michigan-Brookhaven (IMB) (Bionta et al. 1987) and Baksan (Alekseev et al. 1987), almost at the same time. So far, this is the only time that astronomers have observed neutrinos from a newborn compact object. In this paper, we investigate whether the cooling behavior of an SS can match observations of the SN 1987A neutrino burst.

This paper consists of the following parts. The study of the entire thermal evolution of a newborn SS is presented in Section 2, which includes calculations of the internal energy of a newborn SS with different masses in Section 2.1, radiation of the proto-SS in Section 2.2, and the specific thermal evolution and phase transition in Section 2.3. After the theoretical calculations we describe the neutrino burst from SN 1987A and reproduce it with our model in Section 3. Finally Section 4 highlights the conclusions we have reached as well as some discussions.

2 THERMAL EVOLUTION OF A NEWBORN STRANGEON STAR

Huge internal energy is stored in a newborn SS after collapse, and then the energy is released by photons and neutrinos. This process is dominated by neutrino radiation. During this cooling process a sharp drop in temperature leads to a phase transition in the SS. In this section, we make a rough calculation about this evolution process.

2.1 Internal Energy

Different from hadron stars and hybrid stars bounded by gravity, an SS is a self-bounded object that is bounded by residual color-interactions between strangeons. Correspondingly, the equation of state, which is distinctly reflected in $M - R$ relations, varies in different models. The $M - R$ relations of gravitationally bound neutron stars have been proposed by many authors (Müther et al. 1987; Prakash et al. 1988; Akmal & Pandharipande 1997; Glendenning & Schaffner-Bielich 1999), and the results showed that a more massive neutron star might correspond to a smaller radius. Generally, a mass higher than $2\,M_\odot$ is difficult to explain in these models, but this is natural in the SS model. The main reasons are the different mass density gradient from stellar center to its surface and the fact that strangeon matter can have a stiff equation of state due to strong coupling (Guo et al. 2014).

Mass density ρ consists of rest-mass density and energy density which, for an SS, reads,

$$\rho = n_{\rm s}(N_{\rm q}m_0 + E/c^2), \tag{1}$$

where $n_{\rm s}$ is the number density of strangeons, m_0 is the constituent quark mass and $N_{\rm q}$ is a free parameter which is related to the number of quarks in each strangeon. As mentioned in Section 1, we take $N_{\rm q} = 6 \sim 18$ for each strangeon. Energy density, E, in Equation (1) contributes little to the mass density (Guo et al. 2014) in our model, so it is ignored in the following calculations but is significant for the equation of state. On the surface, the density could approximate the rest-mass density $\rho_{\rm s} = n_{\rm s}N_{\rm q}m_0$. From the Tolman-Oppenheimer-Volkoff (TOV) equation, the equation of state for SSs can be derived (Lai & Xu 2009; Lai et al. 2013; Guo et al. 2014; Li et al. 2015), and $M - R$ relations can be obtained, as Figure 1 shows. We take two sets of different parameters (the pentagrams shown in Fig. 1) of SSs in the following calculations for indication, including the typical $1.4\,M_\odot$ case and the other of a massive pulsar ($2\,M_\odot$).

When a proto-compact star is formed in the iron core of an evolved massive star, it goes through a transition process that changes gravitational energy (or binding energy $E_{\rm bind}$) into a star's internal energy which is around 10^{53} erg. The gravitational energy would be stored in SS matter as a form of initial thermal energy

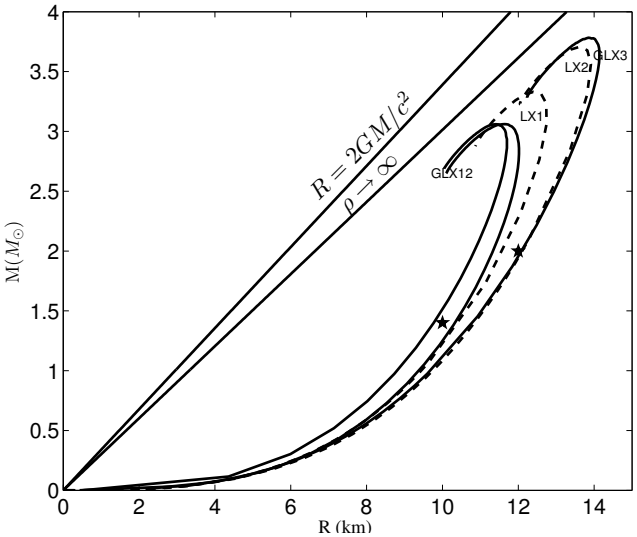

Fig. 1 $M-R$ relations for SSs. The upper black lines show the limits imposed by general relativity and central density. GLX123 (Guo et al. 2014) and LX12 (Lai & Xu 2009; Lai et al. 2013) represent the theoretical $M-R$ relations for SSs. It is clear that the SS model can support a pulsar-like star with a mass of more than 2 $M_\odot$. Since the compact remnant of SN 1987A is still unobservable (Manchester & Peterson 1996; Manchester 2007), no further information can be obtained about its size or mass. In this paper, we parameterize the mass of a newborn SS to be $1.4\,M_\odot$ and $2\,M_\odot$ which are shown as the pentagrams, with corresponding radii of 10 km and 12 km.

(or internal energy) during the strangeonization process. Consequentially, the initial temperature of a proto-SS is extremely high at several 10^{11} K, just like that of a proto-neutron star. In addition to strangeons, degrees of freedom in a proto-SS are uncertain with such high temperature and high density. Migdal did a lot of research on the phase transition of baryons in super-dense stars (Migdal 1972, 1973a,b,c). It indicated that new degrees of freedom, mesons, could be excited due to vacuum instability in a super-dense object. Based on Migdal's arguments, we suggest that a huge number of pions (including π^0, π^+, π^-) would be excited in a newborn SS.

Phenomenologically, pions (with mass $m_{\pi^0} = 134.98\,\mathrm{MeV}$, $m_{\pi^\pm} = 139.57$ MeV) are the lightest carriers of residual strong interactions between strangeons, so they can be excited more easily than other mesons. Other degrees of freedom could be leptons (e.g., neutrinos and positrons) and photons, as well as kinematical oscillation of strangeons. All of these components share the gravitational binding energy and store it as internal energy, which is

$$U = U_{\rm s} + U_{\rm e} + U_{\rm pion} + U_\nu + U_\gamma. \tag{2}$$

For the sake of simplicity, an SS is suggested to have a nearly uniform density from its center to the surface as the previous discussion mentioned. We may approximate an SS as a star with homogenous density of $\rho = 3\rho_0$. If the average number of quarks in a strangeon is 10, then the average mass of strangeons is about 3 times higher than that of a nucleon, $m_{\rm n}$. We can obtain the strangeon number density $n_{\rm s} = \rho/3m_{\rm n}$ and the total number of baryons in a star is $N_{\rm s} = Vn_{\rm s}$. In our model, strangeons behave as classical particles (Xu 2003), so the internal energy of strangeons in an SS is

$$U_{\rm s} = \frac{3}{2}nk\cdot 4\pi\int_0^R r^2 T_r dr, \tag{3}$$

where T_r is the stellar temperature at a point with distance r from the center of the sphere.

Pions are mesons with zero spin. According to Bose-Einstein statistics, the average number of mesons in volume V with momentum between p and $p+dp$ is

$$\frac{4\pi V}{h^3}p^2\frac{dp}{\mathrm{e}^{\frac{\varepsilon-\mu}{kT}}-1}, \tag{4}$$

where the relation between momentum p and energy ε is $\varepsilon^2 = p^2c^2 + m^2c^4$. Considering that there are three kinds of pions, the internal energy carried by pions is

$$U_{\rm pion} = 3\cdot 4\pi\int_0^R\int_{140}^\infty r^2\frac{4\pi}{h^3}\frac{\varepsilon}{\mathrm{e}^{\frac{\varepsilon-\mu}{kT_r}}-1}\frac{\varepsilon\sqrt{\varepsilon^2-m^2c^4}}{c^3}d\varepsilon dr. \tag{5}$$

In a newborn SS, the temperature is so high that the collision frequency between particles is also very high. The system is then almost in a state of thermal equilibrium. On the other hand, the time scale of reaction from neutrino to pion is much longer, thus the system is not in

a state of chemical equilibrium. Therefore, the chemical potential of pions and neutrinos is unequal. In this case, the chemical potential of pions can be approximately treated as the pion's rest mass, $m \sim 140\,\mathrm{MeV}$, so the lower limit of integration in Equation (5) is chosen to be $\varepsilon = 140\,\mathrm{MeV}$.

The dynamic strangeonization process is not completely understood. Whether a newborn SS is isothermal (i.e., temperature gradient negligible if turbulent convention dominates) or non-isothermal (i.e., temperature gradient significant) is uncertain. Both of these assumptions should be considered. So, we can compute the internal energy in both situations: isothermal proto-SSs and non-isothermal proto-SSs. In the case that a newborn SS is an isothermal ball, T_r is independent of r and constant from center to surface. However, considering that heat transfer in the early stage is mainly through neutrino diffusion, a temperature gradient could exist in a proto-SS because neutrinos are opaque, as we prove in Section 2.2. Then T_r should be a function of radius r, and we get the relation between T_r and surface temperature T_s as $T_r \sim T_\mathrm{s}(\frac{R-r}{l})^{1/4}$, which is derived in Section 2.2. With any given surface temperature T_s, we can obtain the corresponding internal energy by the temperature gradient relation.

In order to make a lower energy state for electrons, both the NS model and SS model would go through a process to cancel the electrons by weak interaction. Considering that the number of electrons N_{e^-} is generally around 10^{-5} of the strangeon number N_s, thus U_{e^-} can be ignored. We also ignore U_ν (and U_{e^+}) and U_γ because these parts contribute little to the total internal energy. The specific calculations will be shown in Section 2.2.

Considering only the components which have dominant contributions to the internal energy, U for both isothermal and non-isothermal cases is shown in Figure 2. It is clear that U of an SS with a different mass is around 10^{53} erg. This result is consistent with the magnitude of binding energy. Comparing the solid lines with the dashed lines, which respectively correspond to U and U_s, we conclude that it is valid to consider pions as an important degree of freedom in a newborn SS.

Our results, shown in Figure 3, suggest that pions share almost half of the gravitational binding energy at initial temperatures which are roughly $40 \sim 50\,\mathrm{MeV}$ for the isothermal case and 10 MeV for the non-isothermal case, according to Equation (5). When the newborn SS cools down, pions will decay rapidly because they are unstable. Then a large amount of neutrinos will be released by pion decay. Therefore, pions would be insignificant, and it would be unnecessary to consider them during the later thermal evolution when T decreases to several MeV, as Figure 3 shows.

2.2 Neutrino Emissivity of a Proto-Strangeon Star

In both neutron stars and SSs, neutrino emission is similar to photon radiation in the early stage (Bethe & Wilson 1985; Janka & Hillebrandt 1989a,b), just like blackbody radiation. It is well known that because neutrinos are less-massive particles, they pass through common substances almost freely because they are only affected by weak interaction with extremely small scattering cross-sections. However, neutrinos produced in a newborn SS can hardly escape freely from inside to the surface because strangeon matter is so dense that the neutrinos are trapped and matter in SSs becomes opaque.

Generally, absorption and scattering are the main mechanisms contributing to neutrino opacity. For the case of free quark matter, absorption processes ($d+\nu_\mathrm{e} \to u+\mathrm{e}^-$, $s+\nu_\mathrm{e} \to u+\mathrm{e}^-$) can play a more significant role in determining the mean free path of the neutrinos than scattering processes ($q+\nu \to q+\nu, q=n,p$). However, in normal nuclear matter, the mean free paths of absorption and scattering processes are almost the same order (Iwamoto 1982). In addition, β equilibrium should have been reached when a newborn SS is formed, thus significant absorption is probably not kinematically allowed in an SS. So, we consider only the scattering process.

Considering that a strangeon is a cluster with a certain number of quarks, it is convenient to take strangeons as special nucleons with strangeness when scattering with neutrinos. In Weinberg's weak interaction theory, Freedman obtained the differential cross section for neutrino-nucleus scattering (Freedman 1974), which reads

$$\frac{d\sigma}{dq^2} = \frac{G^2}{2\pi} a_0^2 A^2 \mathrm{e}^{-2bq^2} \left(1 - q^2 \frac{2ME_\nu + M^2}{4M^2E_\nu^2}\right), \quad (6)$$

where G is the conventional Fermi constant:

$$G = 1.015 \times 10^{-5} m_p^{-2},$$

θ_W is the Weinberg angle,

$$a_0 = -\sin^2\theta_\mathrm{W} \qquad (\sin^2\theta_\mathrm{W} = 0.23 \pm 0.015),$$

A is the nucleon number of the target nucleus and b is related to the target particle radius r by

$$b = \frac{1}{6} r^2 \approx 4.8 \times 10^{-6} A^{2/3}.$$

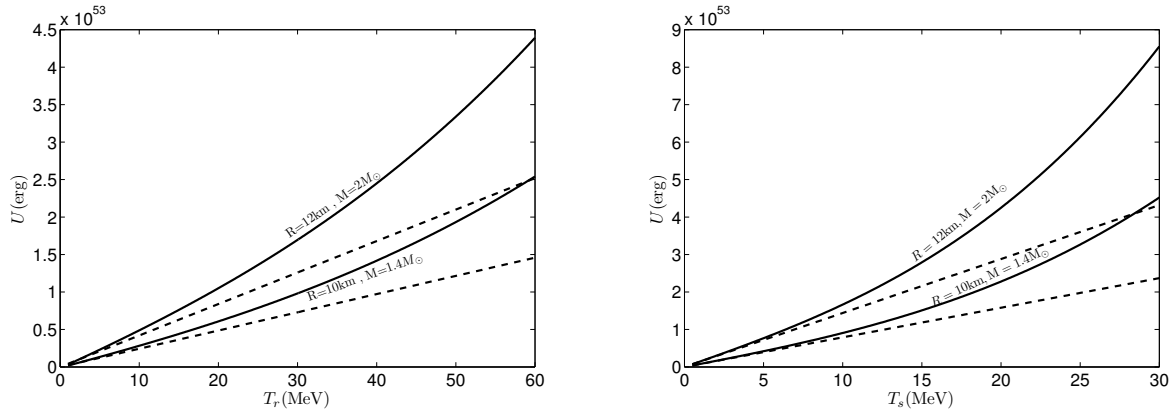

(a) internal energy of isothermal SSs (b) internal energy of non-isothermal SSs

Fig. 2 SSs' internal energy as a function of stellar temperature T. The solid lines mean the total energy U, with mass $2\,M_\odot$ and $1.4\,M_\odot$ from top to bottom respectively. The dashed lines just stand for the corresponding U_s. It is obvious that pions have a great influence on the total internal energy of SSs at high temperature.

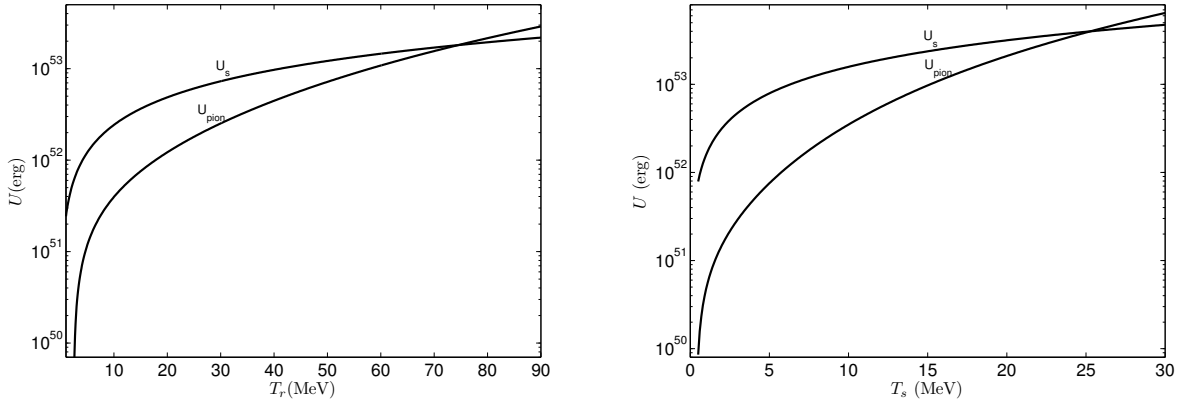

(a) (b)

Fig. 3 A comparison between U_s and U_pion of an SS with $M = 1.4\,M_\odot$ and $R = 10\,\mathrm{km}$. At the beginning, U_pion is almost the same order of magnitude as U_s, or even larger than U_s if the initial temperature is high. As T drops, pions cannot be excited and begin to decay quickly. As we can see from this plot, U_pion reduces rapidly and can be ignored when T drops below several MeV.

Parameter q^2 is the squared momentum transfer. Considering the fact that neutrinos have almost no interaction with the targets, we just take $q \ll E_\nu$, then for supernova neutrinos, the part in brackets is approximately unity with energy $E_\nu \sim 10\,\mathrm{MeV}$ and for strangeons $M \sim 3 \times 10^3\,\mathrm{MeV}$. Integrating Equation (6), one has

$$\sigma \approx 0.03 \times \sigma_0 A^2 \Big(\frac{E_\nu}{m_\mathrm{e}c^2}\Big)^2, \qquad (7)$$

where $\sigma_0 = 1.7 \times 10^{-44}\,\mathrm{cm}^2$. In this case, we can consider a strangeon to be a cluster with baryon number A, and the mean free path of neutrinos in a proto-SS will be $l = (n_\mathrm{sc}\sigma(\nu A))^{-1}$, as we can see in Figure 4.

For a newborn hot SS, the heat transfer before solidification is mainly through neutrino diffusions. As we calculated above, neutrinos in a proto-SS are opaque, so thermal energy delivery will be blocked. Therefore, a temperature gradient could exist in a proto-SS. However, the dynamic process of SS formation is still uncertain, so the effect of temperature gradient may not be ignored. In this section, we take the temperature gradient into consideration and recalculate the cooling process as a contrast to the isothermal case.

Gudmundsson et al. (1982) researched temperature differences between the core and surface. On the surface of a neutron star, photon luminosity can be expressed by $L = 4\pi\sigma T_\mathrm{s}^4 = f(\kappa, T_c)$, where T_s and T_c are surface and central temperature respectively, $f(\kappa, T_\mathrm{c})$ is a function related to the structure and equations of state of a

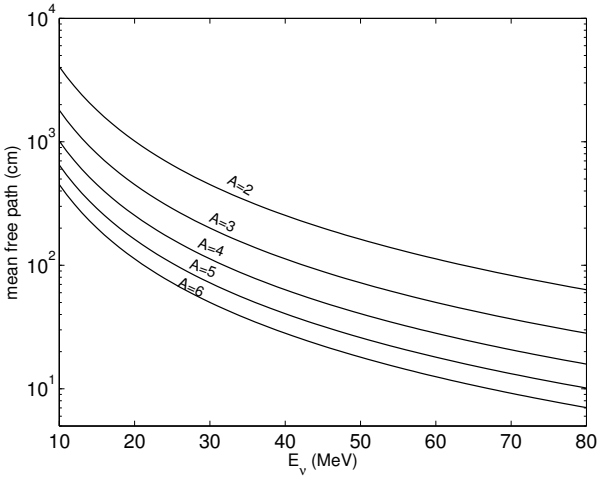

Fig. 4 The mean free path of neutrinos in an SS. We are taking the range of E_ν from 10 MeV to tens of MeV as typical supernova neutrino energies. A strangeon consisting of more quarks with larger A (for example, $A = 6$ means a strangeon with 18 quarks) corresponds to a shorter mean free path. Thus it is hard for neutrinos with high energy to escape from SSs.

neutron star. Similarly, we can obtain a temperature gradient relation in a rough way.

For a proto-SS, we set the internal temperature and surface temperature as T_r and $T_{\rm s}$ respectively, where r is the distance to the center of the proto-SS, and the radius of the star can be set as R. In the ideal situation, if matter is transparent to neutrinos, the theoretically elapsed time for neutrinos at position r is $t_1 \sim (R-r)/c$, and at position R luminosity is of order $R^2T_r^4$. In this case, the whole star shares the same temperature T_r. But, in fact, strangeon matter is opaque to neutrinos at an early stage. Neutrinos can only escape after a number of collisions, which can be thought of as a "random walk" process. Then the number of collisions is $N \sim (R-r)^2/l^2$ where l is the mean free path of neutrinos in a proto-SS. The elapsed time is $t_2 \sim Nl/c \sim (R-r)^2/(lc)$, and the luminosity is of order $R^2T_{\rm s}^4$, so that the process of radiative diffusion has been slowed down to the rate at which energy escapes the proto-SS by a factor $t_2/t_1 \sim (R-r)/l$.

By energy conservation, the delay from the elapsed time leads to temperature gradients in proto-SSs. The internal luminosity, of order $R^2T_r^4$, is reduced to the surface luminosity, of order $R^2T_{\rm s}^4$. Thus $(T_r/T_{\rm s})^4 \sim (R-r)/l$, and we get an estimate of the temperature relation as

$$T_r \sim T_{\rm s}\Big(\frac{R-r}{l}\Big)^{1/4}. \tag{8}$$

The mean free path l is just $(10^{-4} \sim 10^{-3})\ R$, which means that neutrinos can only be emitted freely from a very thin spherical shell on the surface. We can describe this escaping process as bulk emission in comparison with photon radiation, which is also considered as surface emission. Thickness of the emission shell can be regarded as the mean free path l, and we take $l = 10^3$ cm. That is to say, neutrinos below the shell cannot escape immediately. They are trapped in the star and form the so-called "neutrinosphere." The opaque neutrino emission field that appears as surface emission is on the interface below the free emission shell, just like blackbody radiation. In other words, the total luminosity of neutrinos is composed of two parts, bulk neutrino emission luminosity $L_{{\rm b}\nu}$ and surface neutrino emission luminosity $L_{{\rm s}\nu}$. Then we calculate both of them to get the entire neutrino emission luminosity.

At high temperature (such as the case of a newborn SS or neutron star), pair annihilation ($\gamma + \gamma \leftrightarrow {\rm e}^{\pm} \rightarrow \nu + \overline{\nu}$) as described in the framework of Weinberg-Salam theory, is the dominant form of neutrino energy-loss rates as compared to photo-, plasma and bremsstrahlung processes (Itoh et al. 1989). In this case, we only consider this mechanism since we do not exactly know the neutrino energy loss rate of strangeon matter. We often use emissivity in unit volume to calculate neutrino emission energy (Braaten & Segel 1993). The emissivity of a neutrino with high temperature ($T > 1$ MeV) from Itoh et al. (1989) is

$$\begin{aligned}\varepsilon_{\rm pair} \ = \ & 1.809(1+0.104\,q_{\rm pair})f(\lambda)g(\lambda) \\ & e^{-2/\lambda}\ {\rm erg\ s^{-1}\ cm^{-3}},\end{aligned} \tag{9}$$

and

$$\begin{aligned}q_{\rm pair} = & (10.7480\lambda^2 + 0.3967\lambda^{0.5} + 1.0050)^{-1} \\ & \Big[1 + (\rho/\mu_{\rm e})(7.692\times10^7\lambda^3 \\ & +9.715\times10^6\lambda^{0.5})^{-1.0}\Big]^{-0.3},\end{aligned}$$

$$g(\lambda) = 1 - 13.04\lambda^2 + 133.5\lambda^4 + 1534\lambda^6 + 918.6\lambda^8,$$
$$f(\lambda) = \Big[(6.002 \times 10^{19} + 2.084 \times 10^{20}\xi + 1.872 \times 10^2 1\xi^2)e^{-4.9924\xi}\Big] / (\xi^3 + 1.2383/\lambda - 0.4141/\lambda^2)$$

where

$$\lambda = \frac{T}{5.9302 \times 10^9\,\mathrm{K}},$$
$$\xi = \left[\rho\mu_\mathrm{e}^{-1}/(10^9\,\mathrm{g\,cm^{-3}})\right]^{1/3}\lambda^{-1}.$$

In the SS model, the number of electrons per baryon is $< 10^{-4}$ compared to quarks, so we choose the electron mean molecular weight $\mu_\mathrm{e} = 10^5$ in the following calculations. Therefore, the bulk neutrino emission luminosity is

$$L_{b\nu} = 4\pi R^2 l \varepsilon_\mathrm{pair}. \tag{10}$$

Next we consider the surface emission which is similar to blackbody radiation. The "neutrinosphere" below the thin free emission shell can be thought as a neutrino radiation field with radius $R - l \approx R$. In Fermi-Dirac statistics, the emission intensity of neutrinos is

$$I_\nu = \frac{\varepsilon_\nu}{c^2 h^3}\frac{1}{e^{(\varepsilon_\nu - \mu_\nu)/kT} + 1}, \tag{11}$$

where ε_ν is neutrino energy, and the chemical potential $\mu_\nu = 0$. In the radiation field, energy density is

$$u_\nu = \frac{4\pi}{c}\int_0^\infty I_\nu d\varepsilon_\nu = \frac{4\pi(kT)^4}{(hc)^3}F_3, \tag{12}$$

where F_3 is the Fermi integral. The internal energy of a newborn SS is reviewed in Section 2.1. We can then use Equation (12) to estimate $U_\nu \sim 4/3\pi R^3 u_\nu \sim 10^{48}$ erg, and U_γ should be smaller, thus we ignore these two components of the total internal energy in Equation (2). Like photons, the flux of the neutrino radiation is $\frac{c}{4}u_\nu$. Considering three flavors of neutrinos and their antiparticles, it yields

$$L_{s\nu} = 6 \cdot 4\pi R^2 \sigma_v T^4, \tag{13}$$

where $\sigma_v \approx 14.88 \times 10^{-5}$ erg cm^{-2} s^{-1} K^{-4} based on Equation (12).

Another form of radiation that is part of the cooling process is photon radiation. We regard this part as blackbody radiation,

$$L_\gamma = 4\pi R^2 \sigma T^4. \tag{14}$$

The main departure from Equation (14) is that T is the so-called effective temperature T_e in other models. In these models, neutron stars have complex structures, and usually have a crust on the surface (Pethick & Ravenhall 1995) which generates a temperature gradient from the center to the surface, and T_e is generally much lower than 10 MeV, which is the order of surface temperature of a bare newborn SS. In this case, T in Equation (14) is the same as in Equation (13), so the energy released by photons is about 10^{52} erg in our calculation. This energy is more than the total energy needed to drive a supernova (usually 1% of the gravitational binding energy). Chen et al. (2007) did some specific research on the huge energy carried out by photons and found that a supernova may actually be driven by photons.

2.3 Thermal Evolution of a Proto-Strangeon Star with Solidification

The above calculations are aimed at exploring the rapid cooling stage through releasing neutrinos. First we should confirm the internal energy (which equals the binding energy in Section 2.1) and initial temperature of a newborn SS. A simple approximate "empirical formula" describes E_bind well at $M > 0.5\,M_\odot$ (Lattimer & Yahil 1989), and we use it to estimate the binding energy of an SS as

$$E_\mathrm{bind} \simeq 1.5 \times 10^{53}(M/M_\odot)\,\mathrm{erg}. \tag{15}$$

From Equation (15) and the parameters which are $M = 1.4\,M_\odot$ and $M = 2M_\odot$, we can estimate that if an SS is born in SN 1987A, the total thermal energy at the beginning is around 2.1×10^{53} erg and 3×10^{53} erg respectively. Equating the binding energy to the internal energy U in Equation (2), the initial temperatures are respectively $T_\mathrm{r} = 52.9$ MeV, 50.7 MeV (isothermal newborn SSs) and $T_\mathrm{s} = 17.8$ MeV, 16.4 MeV (non-isothermal newborn SSs). So we take $T_\mathrm{r} = 50$ MeV, $T_\mathrm{s} = 18$ MeV for all numerical calculations in this paper.

The internal energy loss rate of an SS at the beginning is

$$-\frac{dU}{dt} = L_{b\nu} + L_{s\nu} + L_\gamma. \tag{16}$$

The evolution which Equation (16) represents lasts during the entire cooling process of normal NSs or SQSs. This process, which is represented by a $T - t$ relation curve with temperature $T > T_\mathrm{m}$, is shown in Figure 6 with different T_m. As mentioned in Section 1, an SS would go through a phase transition from liquid to solid, and this cooling process will not last long. We have assumed that strangeons behave like classical particles, therefore strangeon matter would be localized in a crystal lattice if the stellar temperature reaches its melting temperature T_m, which has a range of 1 MeV

$< T_{\rm m} <$ 6 MeV (Xu 2003; Dai et al. 2011; Lai et al. 2013). The cooling star will remain at a stable temperature ($T = T_{\rm m}$) for a while, and during the stage from liquid to solid, the latent heat would be released through thermal emission. We obtain the time scale of the constant-temperature stage from

$$E' = (L_{\rm b\nu} + L_{\rm s\nu} + L_{\gamma})t. \tag{17}$$

where E' is the latent heat. To estimate the latent heat, we need to know the state of cold quark matter and interactions between strangeons. Lai and Xu (Lai & Xu 2009) used the Lennard-Jones potential to describe the interaction between strangeons and gave the depth of the potential as $V \sim 100$ MeV. Then the latent heat released by each strangeon can be written as $\varepsilon_{\rm s} = fV$, where f is the ratio of potential to melting heat. Based on this work, considering that strangeons are non-relativistic and the interaction is similar to common substances, it is reasonable to estimate f to be $0.01 \sim 0.1$, which is the ratio for most common substances. Then the energy released by each strangeon in the liquid to solid phase can be estimated as $\varepsilon_{\rm s} \sim 1 - 10$ MeV (Dai et al. 2011). The total latent heat of SSs can be written as

$$E' = N_{\rm s}\varepsilon_{\rm s}, \tag{18}$$

and the results are 3×10^{51} erg, 5×10^{51} erg respectively with the corresponding mass $1.4\,M_{\odot}$, $2\,M_{\odot}$ if $\varepsilon_{\rm s} \sim 1$ MeV. When the temperature cools down to the melting temperature which we choose here to be 3 MeV, the values for internal energy U' are 7.2×10^{51} erg and 1.3×10^{52} erg. From the comparison of latent heat and internal energy, it is obvious that most of the internal energy is released in the constant-temperature stage. Due to the uncertainty of many parameters describing latent heat, such as potential and the ratio of potential to melting heat, we use U' to replace E' in Equation (17) to get the time scale for release of latent heat, and results are shown in Figure 5.

Considering the whole process of thermal evolution, the duration of latent heat release is represented by part of the $T - t$ curve, as shown in Figures 6 and 7, which have different melting temperatures.

After this isothermal stage, proto-SSs crystallize immediately and finally become solid. Residual internal energy for SSs in a solid state can be written as

$$U_{\rm re} = \int C_V dT, \tag{19}$$

where heat capacity C_V is comprised of lattice structure component C_V^l and electron component C_V^e, and then $C_V = C_V^l + C_V^e$. Because of the small amount of electrons, C_V^e can be ignored (Yu & Xu 2011). Pions will not be taken into consideration in this part. As mentioned in Section 2.1, Figure 3 shows that when T drops to several MeV, pions decay quickly.

The Debye model is thought to be quite an appropriate method to estimate the specific heat of solid state SSs (Yu & Xu 2011). If a solid medium consists of strangeons, the specific heat is

$$C_V^l = N \cdot \frac{12\pi^4}{5} k \Big(\frac{T}{\theta_D}\Big)^3, \tag{20}$$

where $\theta_D = \hbar(\overline{C_{\rm s}} k_D)/k$ is Debye temperature in which the average sound speed of SSs is $\overline{C_{\rm s}} \sim c$, and D$k_{\rm D} = (6\pi^2 n_{\rm s})^{1/3}$ is the Debye wave number where $n_{\rm s}$ is the number density of strangeons. Because the number density of particles of an SS is extremely high when compared with common substances, the Debye temperature for SSs is as high as 10^{12} K. After crystallization, thermal evolution is represented as

$$-C_V^l \frac{dT}{dt} = L_{\rm b\nu} + L_{\rm s\nu} + L_{\gamma}. \tag{21}$$

Because of the relatively small heat capacity of solid SSs in Equation (21), temperature drops sharply, as shown in Figure 6. A sharp decrease of temperature will lead to an extremely small flux of neutrinos, which means the violent release of neutrinos, i.e. neutrino burst, will cut off after the phase transition.

By combining Equations (16), (17) and (21) the whole cooling process of proto-SSs can be modeled, which is plotted in Figures 6 and 7. Temperature decreases in this process mostly result from neutrino emission, and this process corresponds to the detected neutrino burst. The specifics will be discussed below.

3 THE NEUTRINO BURST OF SN 1987A IN A STRANGEON STAR MODEL

A neutrino burst is an astronomical phenomenon that occurs during the fast cooling stage of a newborn compact star in a supernova. If an SS is born in SN 1987A, the neutrino burst should be explained by the SS model. In this section, we test the thermal evolution of proto-SSs we studied in Section 2.2 and Section 2.3, by the SN 1987A neutrino burst.

3.1 Neutrino Burst Events associated with SN 1987A

The SN 1987A neutrino burst was detected at three locations (Hirata et al. 1987, 1988; Bionta et al. 1987; Bratton et al. 1988; Alekseev et al. 1987; Loredo & Lamb 2002),

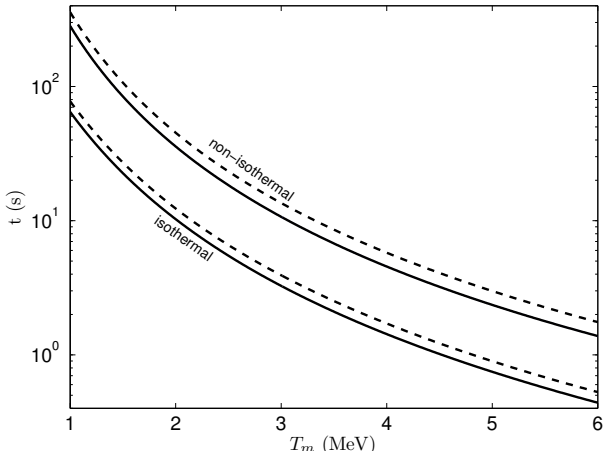

Fig. 5 Time scale of the constant-temperature stage of the phase transition process. The dashed curves have parameters $M = 2\,M_\odot$, $R = 12\,$km, and the solid curves correspond to $M = 1.4\,M_\odot$, $R = 10\,$km. The curves on the top are the time scale of proto-SSs with temperature gradient, and the curves below correspond to isothermal proto-SSs. It can be seen that the duration of the isothermal stage is highly sensitive to melting temperature.

Table 1 Properties of the detected neutrino burst events associated with SN 1987A. Events K1, K2,..., K16 were detected by Kamiokande-II, and I1, I2, ..., I8 and B1, B2, ..., B5 were recorded by IMB and Baksan respectively. Relative time here means the starting moment of each detector's first event, and does not represent the absolute starting time of the neutrino burst.

Detector	Relative time (s)	Energy (MeV)	Detector	Relative time (s)	Energy (MeV)
K1	0	20.0±2.9	I1	0	38±7
K2	0.107	13.5±3.2	I2	0.412	37±7
K3	0.303	7.5±2.0	I3	0.650	28±6
K4	0.324	9.2±2.7	I4	1.141	39±7
K5	0.507	12.8±2.9	I5	1.562	36±9
K6	0.686	6.3±1.7	I6	2.684	36±6
K7	1.541	35.4±8.0	I7	5.010	19±5
K8	1.728	21.0±4.2	I8	5.582	22±5
K9	1.915	19.8±3.2			
K10	9.219	8.6±2.7			
K11	10.433	13.0±2.6			
K12	12.439	8.9±2.9	B1	0	12.0±2.4
K13	17.641	6.5±1.6	B2	0.435	17.9±3.6
K14	20.257	5.4±1.4	B3	1.710	23.5±4.7
K15	21.355	4.6±1.3	B4	7.687	17.5±3.5
K16	23.814	6.5±1.6	B5	9.099	20.3±4.1

and all relevant neutrino events observed are listed in Table 1.

With different energy thresholds, these three detectors recorded different numbers of neutrino events. The energy threshold of Kamiokande-II was 7.5 MeV, and in early data, events K6, K13, K14, K15 and K16 were not included. However, these five neutrinos were picked up from the neutrino background and were found to be associated with this neutrino burst in subsequent analyses (Loredo & Lamb 2002; Vissani 2015). The energy thresholds of other detectors were 15 MeV for IMB and 10 MeV for Baksan. With lower energy threshold, Kamiokande-II could detect many more events than the other two, as shown in Table 1.

It is difficult to determine exactly when the neutrino burst began. Considering the uncertainty in universal time, the first event observed by Kamiokande-II, IMB and Baksan occurred at 7:34:35 UT∼7:36:35

UT, 7:35:40.95 UT∼7:35:41.05 UT, and 7:35:18 UT∼7:36:14 UT respectively (Aglietta et al. 1990). In this situation, a separate analysis of these three groups of data may be more accurate when researching a time-dependent physical process, such as $T-t$ evolution of proto-NSs or proto-SSs.

3.2 Understanding the Neutrino Burst Events in the Strangeon Star Cooling Model

When discussing the time-dependent cooling process of SSs and testing the model with the observed events, it is obviously unsuitable to perform a combined analysis on all data together. Because of the aforementioned uncertainty in universal time between three laboratories, the exact moments of the first event of the three detectors were uncertain. For this reason, data from three different timelines cannot be analyzed by sharing a common starting time. For the sake of preciseness and objectiveness, we decided to chose Kamiokande-II's events as the optimal sample, without a combined analysis that includes IMB and Baksan.

The relation between neutrino energy and stellar temperature can be derived from the neutrino distribution function $f = E_\nu^2/(1+\exp(E_\nu/T))$, where T is the temperature of SSs in our model. Then the mean energy can be obtained as (Janka & Hillebrandt 1989b)

$$\langle E_\nu \rangle = \frac{\int_0^\infty E_\nu f dE_\nu}{\int_0^\infty f dE_\nu} \approx 3.15T. \qquad (22)$$

We use relations $E_\nu \sim 3.15T$ to represent the neutrinos' energies with SS's temperature, and investigate these 15 time-dependent events (without event K1) together with the $T-t$ evolution. In this case, the theoretical cooling curves of proto-SSs calculated in Section 2 can be tested by the 15 observed neutrino events.

For the $T-t$ curves, we take melting temperature to be $T_{\rm m}$=6, 3, 1.5 MeV for isothermal SSs, and $T_{\rm m}$ =3, 2.5, 2 MeV for non-isothermal SSs. Each $T_{\rm m}$ corresponds to a different lasting-time of the phase transition. For comparison, we give the cooling curve of a normal proto-NS with mass $1.4\,M_\odot$ at the same stage. The results are shown in Figure 6. In Figure 7 we also present another two $T-t$ relations which correspond to SSs with different masses. Because the normal NS model cannot support compact stars having more than $2\,M_\odot$ (not including a black hole), there is no comparison shown in Figure 7.

It appears that there is almost no difference between $T-t$ relations for $M=1.4\,M_\odot, R=8$ km. This indicates that a neutrino burst is a good way to examine the different pulsar-like object models, but not a good way to investigate the $M-R$ relation. However, all these results show that our solid SS model with a melting temperature around 1 MeV can reproduce the neutrino burst well, which can be explained by observations.

4 CONCLUSIONS AND DISCUSSION

In this paper, comprehensive calculations are made on the entire thermal evolution of a newborn SS, including its thermal energy, radiation and phase transition. Our conclusions are as follows.

(1) Pion excitation can greatly contribute to the internal energy, as shown in Figure 3. The total thermal energy of pions and strangeons is in accordance with the fundamental core collapse theories of a massive star.
(2) The theoretically time-dependent temperature evolution of an SS model, for both isothermal and non-isothermal cases, coincides well with the SN 1987A neutrino burst when compared with the normal neutrino-driven NS model, as indicated in Figures 6 and 7. It is worth noting that there is an obvious cut-off of the neutrino burst after the liquid-solid phase transition occurs in our model. The cut-off time becomes longer if the melting temperature is lower, and/or if the temperature gradient is more significant. A long neutrino burst during explosion would not be good for a successful supernova in a normal neutron star model, but does not matter in the SS model because the explosion is photon-driven rather than neutrino-driven (Chen et al. 2007).

The characteristic cut-off of the neutrino burst in the model indicates that almost no supernova neutrinos can be detected after the liquid-solid phase transition, i.e., the solidification of strangeon matter. The extremely low flux of neutrino emission (with final neutrino energy around 3 MeV) makes it difficult for the detector to record consecutive neutrino events. However, in case of NS models without neutrino cut-off, a detector would be able to detect a large number of supernova neutrinos continuously even if the neutrino energy is lower than 3 MeV. Therefore, this aspect would be a way to test those two kinds of models by future advanced neutrino detectors. New neutrino experiments are already underway with many planned for the near future. For example, Jiangmen Underground Neutrino Observatory (JUNO) could record thousands of neutrino events or more during a supernova like SN 1987A (An et al. 2016). If more events can be detected, more information would be available related to the compact remnant, and we are looking

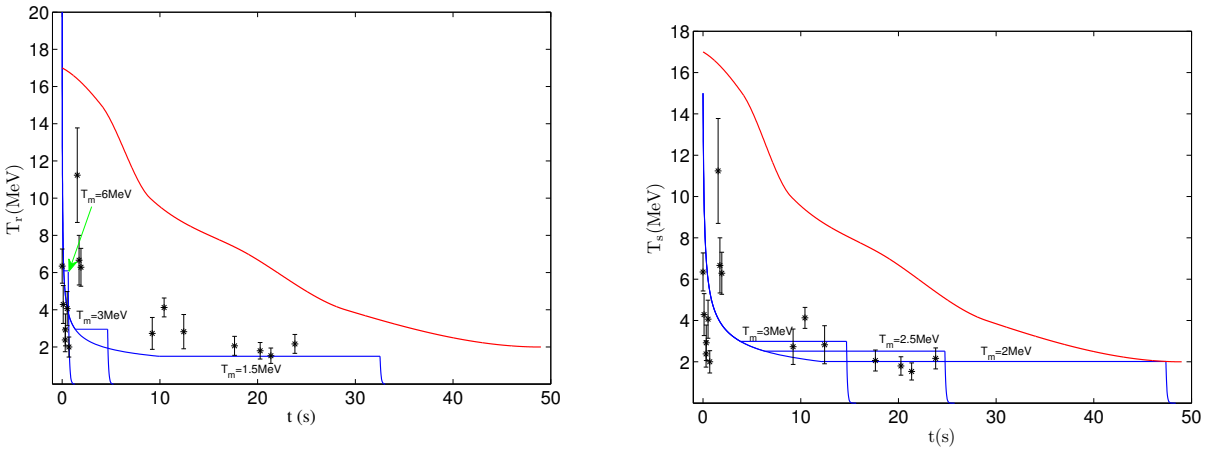

(a) Cooling process for isothermal proto-SSs

(b) Cooling process for non-isothermal proto-SSs

Fig. 6 This is the T-t relation of a proto-SS with $M = 1.4\,M_\odot, R = 10\,\mathrm{km}$. Both in panels (a) and (b), the upper red curve is the cooling process of a normal proto-NS (with mass $M' = 1.4\,M_\odot$) taken from Pons et al. (1999). The 15 black dots with error bars are 15 neutrino events, for which the neutrino energy has been represented by proto-SSs' temperature with the relation $E_\nu = 3.15T$. It can be seen that T in a proto-SS drops rapidly in the early stage, and then the star will stay isothermal during phase transition, as the straight lines indicate. After phase transition, solid SSs cool more drastically than before. In this case, consequently, the emission intensity decreases quickly, hence leading to a cut-off in this neutrino burst. By contrast, normal NSs cool down smoothly all the time and the concomitant neutrino burst has no obvious termination in several tens of seconds. The results indicate that if the proto-SS can be thought of as an isothermal ball, the melting temperature $T_\mathrm{m} \sim 1\,\mathrm{MeV}$ coincides well with the neutrino burst events. Taking the temperature gradient into consideration, $T_\mathrm{m} \sim 2$ would be acceptable. Both of these two situations can roughly fit the neutrino bust.

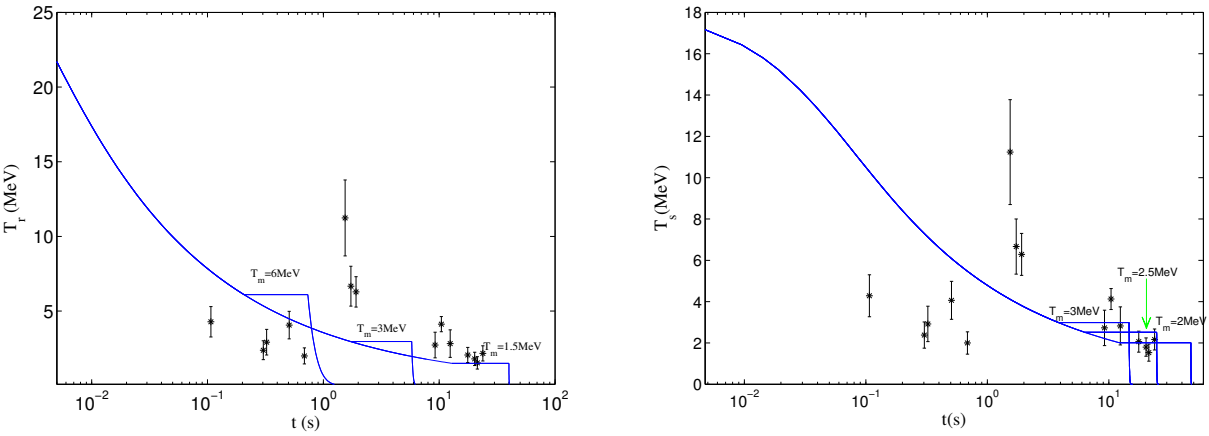

(a)

(b)

Fig. 7 $T - t$ relations of SSs for $M = 2\,M_\odot, R = 12\,\mathrm{km}$. The curves in (a) and (b) represent the logarithm of t, to show more details about the early cooling stage.

forward to detecting supernova neutrino bursts as well as to testing the models.

However, in the extremely early stage of the cooling process, which corresponds to the high temperature part and the time-dependent temperature evolution in an early stage (before phase transition), some aspects need further discussions. Certainly less neutrino events were recorded in this very early stage than the later cooling process, as shown in Table 1 and Figure 6. We will discuss both the technical and theoretical aspects of this issue as follows.

Technically, each of the three detectors has a limit to its trigger rate, which makes it hard to record at a millisecond interval. For example, the IMB detector is dead for about 35 ms after each trigger, which is of the same order as Kamiokande-II (Bionta et al. 1987). Moreover, the total number of photoelectrons per event

in the Kamiokande-II photomultiplier tubes had to be less than 170, corresponding to a maximum electron energy of 50 MeV (Hirata et al. 1988). In addition, due to uncertainty in universal time between those detectors (K, I and B in Table 1), we cannot adopt all of the data at the same initial time, and therefore Kamiokande events are shown in Figure 6.

Theoretically, we have not considered the interaction between neutrinos and circumstellar matter around a newborn SS. A neutrino's mean free path could be much smaller than the length scale if one takes the enclosed mass of a core collapse supernova as high as $0.4\,M_{\odot}$ (in milliseconds after supernova explosion, Roberts & Reddy 2016). One may then expect that the time of arrival and spectrum of supernova neutrinos should be modified if this circumstellar matter effect is included.

Acknowledgements This work is supported by the National Natural Science Foundation of China (11673002, U1531243 and 11373011) and the Strategic Priority Research Program of CAS (No. XDB23010200).

References

Aglietta, M., Badino, G., Bologna, G., Castagnoli, C., & Castellina, A. 1990, Nuovo Cimento C Geophysics Space Physics C, 13, 365

Akmal, A., & Pandharipande, V. R. 1997, Phys. Rev. C, 56, 2261

Alekseev, E. N., Alekseeva, L. N., Volchenko, V. I., & Krivosheina, I. V. 1987, Soviet Journal of Experimental and Theoretical Physics Letters, 45, 589

An, F., An, G., An, Q., et al. 2016, Journal of Physics G Nuclear Physics, 43, 030401

Antoniadis, J., Freire, P. C. C., Wex, N., et al. 2013, Science, 340, 448

Bethe, H. A., & Wilson, J. R. 1985, ApJ, 295, 14

Bionta, R. M., Blewitt, G., Bratton, C. B., Casper, D., & Ciocio, A. 1987, Physical Review Letters, 58, 1494

Braaten, E., & Segel, D. 1993, Phys. Rev. D, 48, 1478

Bratton, C. B., Casper, D., Ciocio, A., et al. 1988, Phys. Rev. D, 37, 3361

Chen, A., Yu, T., & Xu, R. 2007, ApJ, 668, L55

Dai, S., Li, L., & Xu, R. 2011, Science China Physics, Mechanics, and Astronomy, 54, 1541

Demorest, P. B., Pennucci, T., Ransom, S. M., Roberts, M. S. E., & Hessels, J. W. T. 2010, Nature, 467, 1081

Freedman, D. Z. 1974, Phys. Rev. D, 9, 1389

Glendenning, N. K., & Schaffner-Bielich, J. 1999, Phys. Rev. C, 60, 025803

Guo, Y.-J., Lai, X.-Y., & Xu, R.-X. 2014, Chinese Physics C, 38, 055101

Hirata, K., Kajita, T., Koshiba, M., Nakahata, M., & Oyama, Y. 1987, Physical Review Letters, 58, 1490

Hirata, K. S., Kajita, T., Koshiba, M., et al. 1988, Phys. Rev. D, 38, 448

Itoh, N., Adachi, T., Nakagawa, M., Kohyama, Y., & Munakata, H. 1989, ApJ, 339, 354

Iwamoto, N. 1982, Annals of Physics, 141, 1

Janka, H.-T., & Hillebrandt, W. 1989a, A&AS, 78, 375

Janka, H.-T., & Hillebrandt, W. 1989b, A&A, 224, 49

Lai, X. Y., Gao, C. Y., & Xu, R. X. 2013, MNRAS, 431, 3282

Lai, X. Y., & Xu, R. X. 2009, MNRAS, 398, L31

Lai, X.-Y., & Xu, R.-X. 2016a, RAA (Research in Astronomy and Astrophysics), 16, 46

Lai, X.-Y., & Xu, R.-X. 2016b, Chinese Physics C, 40, 095102

Lattimer, J. M., & Yahil, A. 1989, ApJ, 340, 426

Li, Z., Qu, Z., Chen, L., et al. 2015, ApJ, 798, 56

Loredo, T. J., & Lamb, D. Q. 2002, Phys. Rev. D, 65, 063002

Manchester, R. N. 2007, in American Institute of Physics Conference Series, 937, Supernova 1987A: 20 Years After: Supernovae and Gamma-Ray Bursters, ed. S. Immler, K. Weiler, & R. McCray, 134

Manchester, R. N., & Peterson, B. A. 1996, ApJ, 456, L107

Migdal, A. B. 1972, Soviet Journal of Experimental and Theoretical Physics, 34, 1184

Migdal, A. B. 1973a, Nuclear Physics A, 210, 421

Migdal, A. B. 1973b, JETP Letters, 36, 1052

Migdal, A. B. 1973c, Physical Review Letters, 31, 257

Müther, H., Prakash, M., & Ainsworth, T. L. 1987, Physics Letters B, 199, 469

Pethick, C. J., & Ravenhall, D. G. 1995, Annual Review of Nuclear and Particle Science, 45, 429

Pons, J. A., Reddy, S., Prakash, M., Lattimer, J. M., & Miralles, J. A. 1999, ApJ, 513, 780

Prakash, M., Lattimer, J. M., & Ainsworth, T. L. 1988, Physical Review Letters, 61, 2518

Roberts, L. F., & Reddy, S. 2016, arXiv:1612.03860

Thompson, T. A., Burrows, A., & Pinto, P. A. 2003, ApJ, 592, 434

Tong, H. 2016, Science China Physics, Mechanics, and Astronomy, 59, 5752

Vissani, F. 2015, Journal of Physics G Nuclear Physics, 42, 013001

Wang, W., Lu, J., Tong, H., et al. 2017, ApJ, 837, 81

Xu, R. X. 2003, ApJ, 596, L59

Xu, R. X., Tao, D. J., & Yang, Y. 2006, MNRAS, 373, L85

Yu, M., & Xu, R. X. 2011, Astroparticle Physics, 34, 493

Zhou, E. P., Lu, J. G., Tong, H., & Xu, R. X. 2014, MNRAS, 443, 2705